

Research Papers

# The influence of additives on the growth kinetics and mechanism of L-alanine crystals

David Lechuga-Ballesteros<sup>1</sup>, Naír Rodríguez-Hornedo<sup>\*</sup>

*College of Pharmacy, The University of Michigan, Ann Arbor, MI 48109–1065, USA*

Received 25 June 1993; modified version received 12 July 1994; accepted 19 July 1994

---

## Abstract

Results for the characterization of the growth kinetics and mechanism of L-alanine crystals, grown from aqueous solution in the presence and absence of tailor-made additives are reported. L-Alanine crystals grown from water in the absence of additives are prismatic, elongated along the crystallographic *c*-axis bounded by the {120}, {010}, {110}, {210} and {011} faces. The growth rate of L-alanine crystals was measured by monitoring the change of size of individual crystals as a function of time. Examination of both the growth rate dependence on supersaturation and the structure of the crystal surface, reveals that the {120}, {010}, and {011} crystal faces of L-alanine grow following the spiral growth mechanism, both in the presence and absence of additives. This mechanism was confirmed by examining the surface topography of crystals by atomic force microscope. The growth rate of L-alanine crystals in the presence of L-leucine and L-phenylalanine at concentrations as low as 0.02 *m* (i.e., 0.3 g additive/100 g solvent or 0.18 g additive/100 g L-alanine) is drastically reduced and the crystals are bounded by the {120} and {011} faces. The inhibitory effect of these additives is explained by a Langmuir isotherm, assuming that the inhibition of the growth rate is proportional to the degree of surface coverage and that the crystal surface is homogeneous with respect to the energy of adsorption sites.

**Keywords:** L-Alanine; Crystal growth mechanism; Additive effect; Additive adsorption; Amino acid; Atomic force microscope

---

## 1. Introduction

The presence of additives in small amounts may greatly influence the crystallization kinetics of organic compounds from solution. An additive may affect both the activity of the crystallizing

solute in solution and interfere with the crystal growth process through adsorption onto the growing surface. Additives that closely resemble the chemical structure of the crystallizing solute, such additives, referred to as 'tailor-made additives' (Addadi et al., 1985), offer a means of selectively modifying the crystal habit through adsorption onto the growing-crystal surface. An important, direct application of these concepts, that explain the effect of additives on crystal growth, can be used to aid in the design of

---

<sup>\*</sup> Corresponding author. Tel. (313)-763-0101.

<sup>1</sup> Present address: Abbott Laboratories, Product Development, D-496, 1401 Sheridan Road, North Chicago, IL 60064, U.S.A.

crystalline drugs with the desired physicochemical properties. These properties include: crystal morphology, size, lattice energy, solubility and rate of dissolution.

The characterization of the growth kinetics and mechanism of L-alanine crystals from aqueous solutions containing small concentrations of L-leucine and L-phenylalanine is presented. The growth rates of various faces of L-alanine crystals have been evaluated from single crystal measurements at constant supersaturation and temperature. These results are in agreement with the results obtained from crystal size distribution (CSD) measurements during batch crystallization experiments (Lechuga-Ballesteros and Rodríguez-Hornedo, 1993a). Analysis of both the growth rate dependence on supersaturation and the crystal structure has revealed that the growth of the {120}, {010} and {011} L-alanine crystal faces is controlled by integration of the growth units into the crystal surface, and that growth occurs by a defect mediated mechanism. Low concentrations of hydrophobic L-amino acids inhibit the growth rate of L-alanine crystals, but the growth mechanism is not changed. The reduction of the growth rate due to the presence of hydrophobic L-amino acids is associated to a change in crystal morphology induced by a change in the relative growth rate of the different faces of L-alanine crystals. These results are interpreted on the basis of the molecular structure of both the additive species and the crystal structure.

## 2. Experimental

### 2.1. Materials

L-Alanine, L-leucine and L-phenylalanine were purchased from Sigma Chemical Co. (St. Louis, MO), and were used without further purification. Distilled water purified with a Milli-Q water system (Millipore, Bedford, MA) was used.

### 2.2. Crystal growth from single crystal measurements

Growth rates of the {010}, {011} and {120} L-alanine crystal faces were obtained by measur-

ing crystal dimensions at constant supersaturation ( $\ln(C/C_s)$ ) in a flow cell at 25°C. The supersaturation range studied was 0.01–0.10. The concentrations of additive (L-leucine and L-phenylalanine) studied were between 0.15 and 0.60 g additive/100 g solvent (0.09–0.36 g additive/100 g L-alanine). Details of the experimental method are presented in the accompanying paper (Lechuga-Ballesteros and Rodríguez-Hornedo, 1995).

### 2.3. Atomic force microscopy (AFM)

The surface of the different faces of L-alanine crystals, grown in both the presence and absence of additives, was imaged with an Optizoom  $0.8 \times -2.0 \times$  scanning probe microscope attached to a Nanoscope III system (Digital Instruments). This instrument operates in contact mode with an optical lever detection scheme. The cantilevers used (standard silicon nitride with integrated pyramidal tips) were 120  $\mu\text{m}$  long and 22  $\mu\text{m}$  wide.

## 3. Results and discussion

### 3.1. L-Alanine crystal growth from single crystal measurements

#### 3.1.1. Face growth kinetics

Single crystal measurements were performed to measure the face growth rate of individual crystals from flow cell experiments which are useful if growth at constant supersaturation is to be measured, since it is possible to circulate a solution of constant composition, through the crystallization cell, to compensate for the depletion of solute due to crystal growth.

The growth rate measurement process is depicted in Fig. 1. The outline of the crystal is identified at time  $t_1$ , and subsequently at  $t_2$ . The dimensions  $L_1$  (length) and  $L_2$  (width) are recorded and  $\Delta L_i$  is calculated. The growth rate perpendicular to a given face is calculated using the value of the corresponding interfacial angle. The growth rates of the {010}, {120} and {011}

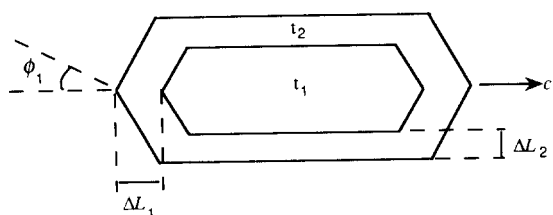


Fig. 1. Single crystal growth rate measurements of L-alanine from flow cell experiments.

faces were calculated using the following equations:

$$R_{(010)} = \frac{1}{2 \sin \phi_1} \left( \frac{dL_1}{dt} \right) \quad (1a)$$

$$R_{(120)} = \frac{1}{2 \sin \phi_2} \left( \frac{dL_2}{dt} \right) \quad (1b)$$

$$R_{(011)} = \frac{1}{2 \sin \phi_3} \left( \frac{dL_2}{dt} \right) \quad (1c)$$

where  $R_{(hkl)}$  is the growth rate perpendicular to the set of faces  $\{hkl\}$  and  $\phi_i$  is the interfacial angle between  $\{hkl\}$  and  $L_i$ . In this case  $\phi_1 = \phi_2 = 46^\circ$  and  $\phi_3 = 56^\circ$ .

The dependence of growth on supersaturation is shown in Fig. 2. The relative magnitude of the observed growth rates is  $R_{(011)} > R_{(120)} > R_{(010)}$ ,

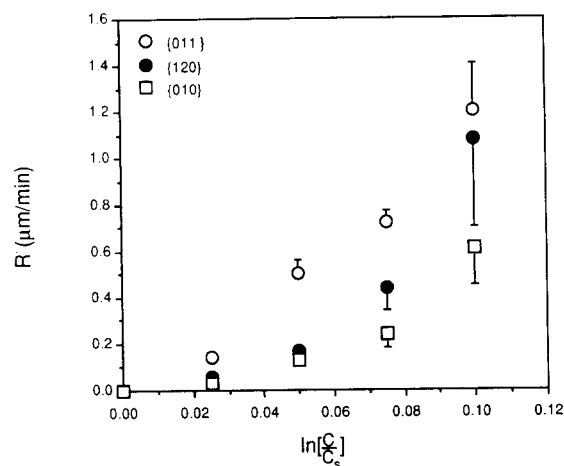


Fig. 2. Growth rate dependence of L-alanine crystal faces on supersaturation. The values shown are average with the standard deviation from the growth rate measurements for six crystals in a flow cell experiment.

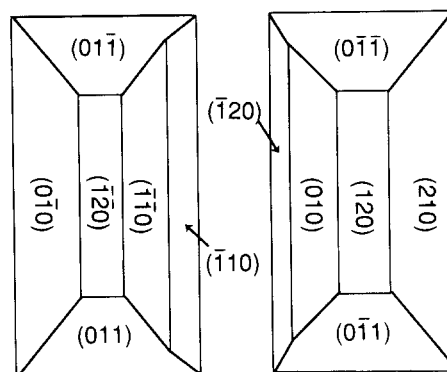


Fig. 3. L-Alanine crystal morphology.

consistent with the morphology of the L-alanine crystals grown from water, since they are elongated along the  $c$ -axis and are bounded by  $\{120\}$  and  $\{010\}$  faces (Fig. 3).

The relative growth rates can be compared to the relative order of the face growth rate predicted from structural considerations as follows. According to the Bravais-Friedel-Donnay-Harker (BFDH) rule (Hartman, 1973), the growth rate of a particular crystal plane is determined by the strength of the bond formed in the growth direction (i.e., perpendicular to the given plane). The strength of the bond can be defined as the energy of attachment,  $E_{att}$ , which is the energy released, when a growth unit is incorporated into the solid phase, as:

$$E_{att} = E_{cryst} - E_{slice} \quad (2)$$

where  $E_{slice}$  is the energy of the bonds of a growth unit with all its neighbors in a connected net of the  $\{hkl\}$  crystal face and  $E_{cryst}$  denotes the total energy of crystallization per growth unit. Then the BFDH rule can be stated as:

$$R_{hkl} \propto E_{att} \quad (3)$$

The strength of the bond is inversely proportional to the interplanar distance,  $d_{hkl}$ . This can be stated as:

$$R_{hkl} \propto \frac{1}{d_{hkl}} \quad (4)$$

The interplanar distance can be calculated from the crystallographic data. For an or-

thorhombic unit cell, as is the case for L-alanine,  $d_{hkl}$  is given by:

$$d_{hkl}^2 = \left( \frac{h^2}{a^2} + \frac{k^2}{b^2} + \frac{l^2}{c^2} \right)^{-1} \quad (5)$$

Symmetry elements in the crystal must be accounted for, since they will determine the effective interplanar distance. The L-alanine crystal lattice is orthorhombic, belonging to the space group  $P2_12_12_1$  with unit cell parameters  $a = 6.023$ ;  $b = 12.343$  and  $c = 5.784$  Å,  $Z = 4$ , as has been determined from X-ray diffraction and neutron diffraction data (Simpson and Marsh, 1966; Lehmann et al., 1972). In this case, the effective interplanar distance for a growth layer along (010) is not 12.343 but 6.172 Å, as if it were a (020) plane, because of the screw axis along the  $b$ -crys-

Table 1

Interplanar distances calculated according to Eq. 5

Plane	Interplanar distances	
	$d(hkl)$ Å	$1/d(hkl)^2$
{010}	12.343	0.00656
{020}	6.172	0.02625
{110}	5.413	0.03413
{120}	4.310	0.05383
{210}	2.926	0.11680
{011}	5.237	0.03646

tallographic direction, as determined by the symmetry elements of the  $P2_12_12_1$  space group. These results are summarized in Table 1. According to Eq. 4, the relative growth rates are expected to be  $R_{\{120\}} > R_{\{011\}} > R_{\{010\}}$ . Unless the growth mechanisms of the different faces are

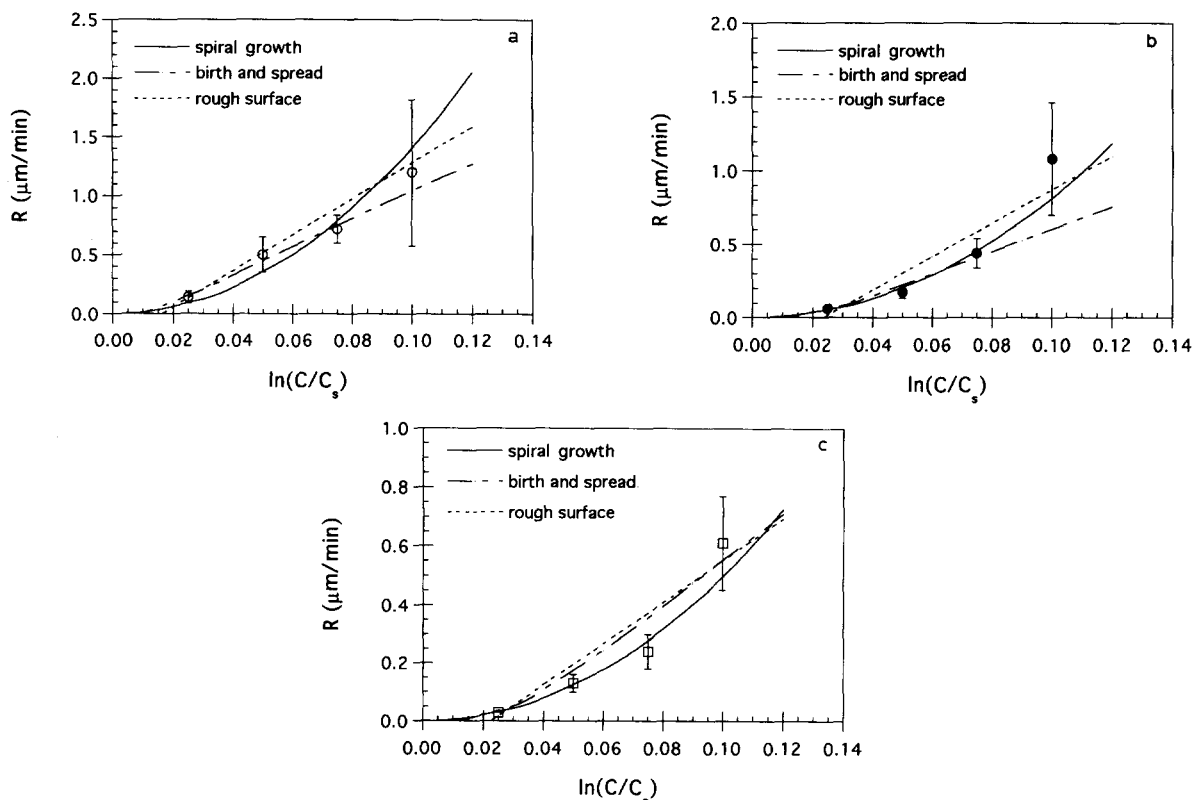


Fig. 4. Predicted and observed L-alanine growth rate dependence on supersaturation for (a) {011}, (b) {120} and (c) {010} faces from single crystal measurements.

different, the lack of agreement with the observed growth rates must be related to some interaction between the solvent and the crystal faces, which are not considered in the empirical model described by Eq. 4.

### 3.2. Growth mechanism of the different faces of L-alanine crystals

The mechanism controlling the incorporation of growth units to the crystal lattice may be understood by analyzing the growth rate dependence on supersaturation. In Fig. 2,  $R_{(hkl)}$  is found to have a strong dependence on supersaturation for the three sets of faces measured.

When crystal growth is governed by surface integration two mechanisms can be considered: rough surface and step formation (Chernov, 1989). In the latter, the source of steps is dislocations or surface nuclei. If growth is not limited by the step diffusion on the surface, i.e., there are so many active sites available for crystal growth that the collision of a growth unit with the surface is most likely to result in incorporation into the crystal lattice, then growth occurs by the rough surface mechanism. This predicts the growth rate  $R$  to be proportional to the driving force  $\sigma$ :

$$R = K_{RS}\sigma \quad (6)$$

where  $K_{RS}$  is a proportionality constant.

If growth is controlled by screw dislocations (Burton et al., 1951) then it follows the spiral growth mechanism, defined as:

$$R = k_1 T \sigma^2 \tanh\left(\frac{k_2}{T\sigma}\right) \quad (7)$$

where  $k_1$  and  $k_2$  are constants.

If the growth is controlled by the formation of two-dimensional nuclei on the surface of the growing crystal to which the growth units are attached, then the growth kinetics is described by the birth and spread mechanism:

$$R = K_{SN}\sigma^{5/6} \exp\left(-\frac{\pi\gamma^2}{(kT)^2\sigma}\right) \quad (8)$$

where  $\gamma$  is the interfacial energy and  $k$  represents the Boltzmann constant.

The different growth models were fitted to the observed growth rates by weighted non-linear regression. From examining the growth rate dependence of L-alanine crystals on supersaturation (Fig. 4), we conclude that the {120} and {010} L-alanine crystal faces grow by the spiral growth mechanism. The rough surface mechanism leads to rounded crystal faces and in the supersaturation range studied L-alanine crystals exhibited flat faces. However, in the case of the {011} faces it is not clear whether it follows the spiral growth or the birth and spread mechanism from the  $R(\sigma)$  analysis alone. Therefore, it was useful to examine the crystal surface topography to identify the growth mechanism.

### 3.3. Surface structure

The AFM determines surface structure by raster-scanning the sample while the surface is in contact with a small, sharp probe attached to a sensitive cantilever. Surface topography causes deflection of the probe via steric repulsion, which causes bending of the cantilever; this bend can be detected by the change in position of a laser beam reflected off the back of the cantilever onto a position-sensing photodiode. This technique has been recently applied to produce the molecular-level imaging of the crystal surface of different amino acids and to follow the evolution of the molecular surface during dissolution (Manne et al., 1993). Manne et al. (1993) report extended molecularly flat sheets (up to hundreds of nanometers in size) separated by steps a single molecule thick. The ordered lattice of each amino acid could be imaged onto the sheets. Step motion kinetics were also imaged in situ during dissolution of L-leucine in flowing propanol.

In our case, AFM surface imaging was obtained for L-alanine crystals grown in both the presence and absence of additives (Fig. 5). Surface imaging of the {011} crystal faces (Fig. 5 (a)) shows the formation of ordered terraces, characteristic of the spiral growth mechanism, which are comparable to the ones obtained for the {120} and {010} faces. A surface-mediated mechanism has also been reported for small organic molecules, such as sucrose (Albon and Dunning,



Fig. 5. AFM microphotographs of L-alanine crystal grown in flow cell from water at constant supersaturation (0.05) and temperature (25°C). (a) {011} face in the absence of additives (scan rate 10.2 Hz, 0–15 nm resolution) and (b) {120} face in the presence of L-phenylalanine 0.02 *m* (scan rate 10.2 Hz, 0–500 nm resolution)

1962), theophylline (Rodríguez-Hornedo and Wu, 1991), phenytoin (Zipp and Rodríguez-Hornedo, 1992) and glycine (Li and Rodríguez-Hornedo, 1992).

### 3.4. Surface entropy factor, $\alpha$

Predictions of the growth mechanism are often based on thermodynamic considerations. The surface free energy of a compound will determine the roughness, at the molecular level, of the solid liquid interface. This roughness will be related to the energy needed to transfer a solute molecule from the solid phase to the solution bulk. The roughness of the crystal surface (*hkl*) is characterized by the surface entropy factor,  $\alpha_{hkl}$ , defined as (Gilmer and Bennema, 1972):

$$\alpha_{hkl} = \xi_{hkl} \frac{\Delta H_s(T)}{RT} = \xi_{hkl} \frac{\Delta S_s(T)}{R}, \quad (9)$$

where  $\Delta H_s(T)$  is the molar heat of solution and  $\xi_{hkl}$  denotes the dimensionless energy factor given by:

$$\xi_{hkl} = \frac{E_{\text{slice}}}{E_{\text{cryst}}} \approx \frac{n_s}{n_t}, \quad (10)$$

where  $E_{\text{slice}}$  is the energy of the bonds of a growth unit with all its neighbors in a connected net of the (*hkl*) crystal face and  $E_{\text{cryst}}$  represents the total energy of crystallization per growth unit. These energies consist of the bond energies of the crystal without taking the liquid phase into account. The dimensionless energy factor for the (*hkl*) plane can be approximated by the number of bonds with the nearest neighbors in the growth plane,  $n_s$ , to the total number of bonds of a growth unit in the bulk of the crystal  $n_t$ , so:

$$\alpha_{hkl} \approx \frac{n_s}{n_t} \frac{\Delta H_s(T)}{RT}. \quad (11)$$

The dimensionless energy factor can be further approximated by the ratio of the number of bonds with the nearest neighbors in the growth plane,  $n_s$ , to the total number of bonds with the nearest neighbors in the bulk crystal,  $n_t$ . In Eq. 9, changes in the solid-fluid and fluid-fluid interactions directly affect the value of  $\alpha_{hkl}$  and, thus, the predicted growth mechanism. Because  $\alpha_{hkl}$  also includes information specific to a given face, it can be used to predict differences in growth mechanisms of the different faces of a crystal.

Good agreement between known growth mechanisms and calculated  $\alpha_{hkl}$  factor for water

and other systems (Jackson, 1978) has been found, using the criterion that if  $\alpha < 2$ , a rough interface exists and growth is continuous and if  $\alpha > 2$ , the interface is smooth and growth is slower. Successful computer simulations of crystal growth (Bennema and Gilmer, 1973) have been used to determine three approximate growth regimes depending on the value of  $\alpha_{hkl}$  as:

- (i)  $\alpha < 3.2$  indicates a rough interface and continuous growth with no energetic barriers;
- (ii)  $3.2 < \alpha < 4.0$  indicates a smoother interface where the growth mechanism is two dimensional or surface nucleation, and
- (iii)  $\alpha > 4.0$  indicates a microscopically smooth interface with a screw dislocation growth mechanism.

The change in enthalpy due to the solution formation,  $\Delta H_s(T)$ , can be calculated from thermodynamic data using the following equation (Bennema and Van der Eerden, 1987):

$$\frac{d\chi(T)}{dT} \approx \frac{\Delta H_s(T)}{RT^2} \chi(T), \quad (12)$$

where  $\chi$  is the mole fraction of the solute. Alternatively, the heat of melting,  $\Delta H_f(T)$ , can be calculated from the slope of the solubility temperature curve as given by:

$$\ln \chi(T) \approx \frac{\Delta H_f(T_f)}{R} \left( \frac{1}{T} - \frac{1}{T_f} \right) \quad (13)$$

and the heat of solution is given by:

$$\frac{\Delta H_s(T)}{RT} \approx \frac{\Delta H_f(T_f)}{RT_f} - \ln \chi(T). \quad (14)$$

Using the solubility-temperature data available (Bull et al., 1978) for L-alanine, listed in Table 2, a  $\Delta H_s(25^\circ\text{C}) = 7.32 \text{ kJ mol}^{-1}$  ( $1.75 \text{ kcal mol}^{-1}$ ) from Eq. 12, and a  $\Delta H_s(25^\circ\text{C}) = 7.95 \text{ kJ mol}^{-1}$  ( $1.90 \text{ kcal mol}^{-1}$ ) from Eq. 14 were calculated.

Using the value of  $\Delta H_s(T)$  calculated from Eq. 12, a value for  $\Delta H_s(T)/RT = 3.0$  is obtained, thus from Eq. 11 we obtain:

$$\alpha_{hkl} \approx \frac{n_s}{n_t} (3.0) \quad (15)$$

Since  $\xi_{hkl}$  is expected to be less than unity, as  $n_t > n_s$ , then all  $\alpha_{hkl}$  values for L-alanine are

Table 2

Solubility of L-alanine at various temperatures (after Bull et al., 1978)

$T$ ( $^\circ\text{C}$ )	Solubility ( $m$ )	$\chi_{\text{sol}} (\times 10^2)$	$\Delta H_s(298)$ ( $\text{kJ mol}^{-1}$ )
20.0	1.744	3.044	
25.0	1.839	3.203	7.32 (0.29) <sup>a</sup>
29.8	1.940	3.373	

$\chi_{\text{sol}}$ , L-alanine mole fraction;  $\Delta H_s(298)$ , heat of solution at 298 K (from Eq. 12) ( $\Delta H_s(298) = 7.95 \text{ kJ mol}^{-1}$  from Eq. 14).

<sup>a</sup> Standard deviation.

expected to be less than 3. Using the criteria above, according to the range for  $\alpha_{hkl}$  values established from computer simulations L-alanine is expected to grow by a rough mechanism. This is not the case for L-alanine as it was shown above from the  $R(\sigma)$  data and AFM photomicrographs.

In the case of glycine, the  $E_{\text{slice}}$  and  $E_{\text{cryst}}$  values have been obtained from energy calculations (Weissbuch et al., 1983) and the values for the surface entropy factor are  $\alpha_{010} = 5.5$  and  $\alpha_{011} = 3.9$  (Li and Rodríguez-Hornedo, 1992). According to the criteria for the  $\alpha_{hkl}$  values the growth of the {010} faces of glycine crystals should be governed by the screw dislocation mechanism, and that of the {011} by the surface nucleation mechanism. However, from  $R(\sigma)$  the growth of {010} and {011} was determined to be governed by the screw dislocation mechanism (Li and Rodríguez-Hornedo, 1992). The lack of agreement between the thermodynamic and kinetic predictions were explained in terms of the interaction between the solvent molecules and the {011} faces of glycine crystals, which are very similar in chemical structure to the {011} planes of L-alanine. Upon examining the structure of the crystal face it was concluded that the hydrophilic nature of these faces was responsible for their enhanced interaction with water molecules.

A successful prediction of the growth mechanism through the  $\alpha_{hkl}$  factor was found in phenytoin. The surface entropy factor was calculated according to Eq. 11, with  $\xi_{hkl} = 0.5$ , calculated from the number of bonds at the surface and in the bulk of the crystal, to be  $\alpha_{hkl} = 6.5$ , i.e., growth mediated by screw dislocations is ex-

Table 3  
Solubility and heat of solution at 25°C for various compounds

Compound	Solubility ( <i>m</i> )	$\chi_{\text{sol}} (\times 10^2)$	$\Delta H_s(298)$ (kJ mol <sup>-1</sup> )	$\Delta H_s(298)/RT$
Glycine	3.330	5.654	14.23 <sup>a</sup>	5.7
L-Alanine	1.744	3.203	7.32 <sup>a</sup>	3.0
L-Phenylalanine	0.180	0.323	11.72 <sup>a</sup>	4.7
Phenytoin	$7.592 \times 10^{-5}$	0.020	31.30 <sup>b</sup>	12.6
Sucrose	5.840	9.520	0.60 <sup>c</sup>	0.2

$\chi_{\text{sol}}$ , mole fraction at saturation;  $\Delta H_s(298)$ , heat of solution at  $T = 298$  K;  $R = 8.314$  J mol<sup>-1</sup> K<sup>-1</sup>.

<sup>a</sup> From Greenstein and Winitz (1961).

<sup>b</sup> From Schwartz et al. (1977).

<sup>c</sup> From Mathlouthi and Seuvre (1988).

pected. This is in agreement with the kinetic results (Zipp and Rodríguez-Hornedo, 1992).

From the definition of the surface entropy factor, a relationship between growth mechanism (or surface structure) and the solubility of the compound could be expected, since in general, an increase in solubility is accompanied by a decrease in the  $\Delta H_s(T)$  (see Table 3). This holds true for L-alanine, L-phenylalanine and phenytoin. Furthermore, one could think that, in general, high solubility compounds should grow by a rough surface mechanism as opposed to the low solubility compounds which should be expected to grow by a step mechanism. Glycine, however, is an exception since it is a high solubility com-

pound (3.3 *m*) and yet it has high heat of solution. At the other extreme, sucrose is known to grow through a step mechanism (Dunning et al., 1965) and it has a low heat of solution and a high aqueous solubility, just as in the case of L-alanine. Therefore, we can conclude that the entropy factor,  $\alpha_{hkl}$ , should not be used alone to predict the crystal growth mechanism. Other factors should be taken into consideration, such as association in solution (dimerization is known to occur in the case of glycine) and interactions at the solvent-crystal interface or any kind of interaction able to promote changes in the solution structure. These aspects are discussed in more detail by Davey et al. (1982).

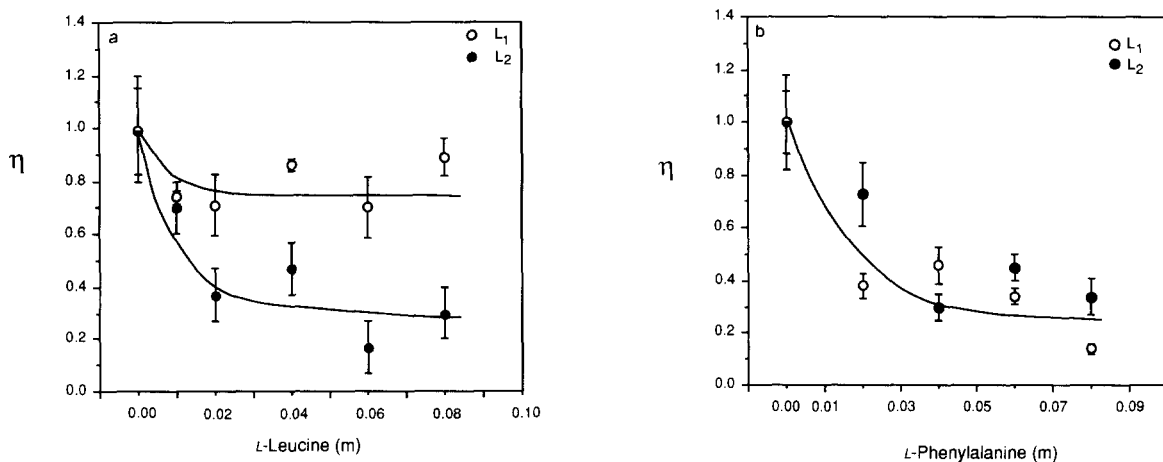


Fig. 6. Effect of (a) L-leucine and (b) L-phenylalanine on the growth rate of L-alanine crystals from single crystal measurements.  $\eta = R_a/R_{\text{max}}$ . Data points reflect the growth rate of the different crystals along their length ( $L_1$ ) and width ( $L_2$ ).  $\sigma = 0.05$ ;  $T = 25^\circ\text{C}$ , flow rate =  $5$  ml  $\text{h}^{-1}$  (using 1/16 inch tubing).



### 3.5. Influence of additives on the growth of L-alanine crystal faces

A series of flow cell experiments were performed at constant supersaturation and temperature ( $\sigma = 0.05$ ;  $T = 25^\circ\text{C}$ ) to assess the effect of L-leucine and L-phenylalanine on the growth kinetics of the different crystal faces of L-alanine. The results obtained from the single crystal measurements are shown in Fig. 6a and b. These graphs show  $\eta = R_a/R_{\max}$  as a function of the concentration of additive in solution.  $R_a$  is the growth rate of L-alanine crystals in the presence of additive and  $R_{\max}$  represents the growth rate in the absence of additives. The growth rate is decreased to a minimum level that can be characterized as the minimal dimensionless growth rate, defined as  $\eta^0 = R_{\min}/R_{\max}$  where  $R_{\min}$  is the minimum growth rate in the presence of the additive. The minimal dimensionless growth rates of L-alanine crystals along both  $L_1$  and  $L_2$  in the presence of L-leucine and L-phenylalanine are summarized in Table 4.

In the case of L-leucine, the inhibition of the growth of the faces associated with  $L_1$  (i.e., {011}) is not as large as that with  $L_2$  (i.e., {120}, {210}, {010} and {110}). When normalized to the face growth rate in the absence of additives the maximum inhibition ( $1 - \eta^0$ ) is greater for  $L_2$  ( $\eta^0 =$

Table 4

Influence of additives on the growth rate of L-alanine (minimal dimensionless growth rates found in the presence of additives)

Additive	Single crystal	
	$\eta_1$	$\eta_2$
L-Alanine	0.70	0.17
L-Phenylalanine	0.14	0.30

0.17) than for  $L_1$  ( $\eta^0 = 0.70$ ). This is consistent with the morphology of L-alanine crystals grown in the presence of L-leucine which are acicular and bounded by the {120} faces.

The presence of L-phenylalanine has a similar effect on the growth of L-alanine crystals, however, the growth along both  $L_1$  and  $L_2$  is affected. In this case the inhibition is greater on  $L_1$  ( $\eta^0 = 0.14$ ) than on  $L_2$  ( $\eta^0 = 0.30$ ). The crystals observed in this case are also acicular, bounded by the {120} faces, and smaller than those crystals grown in the presence of L-leucine.

One important difference, however, is that the growth of L-alanine crystals along the  $c$ -axis is not as drastically inhibited by the presence of L-leucine even at high concentrations. This is reflected in the higher value of  $\eta_1$ . It is interesting to note that, unlike L-leucine, L-phenylalanine does inhibit the growth of the L-alanine crystals along its crystallographic  $c$ -axis. Based on the

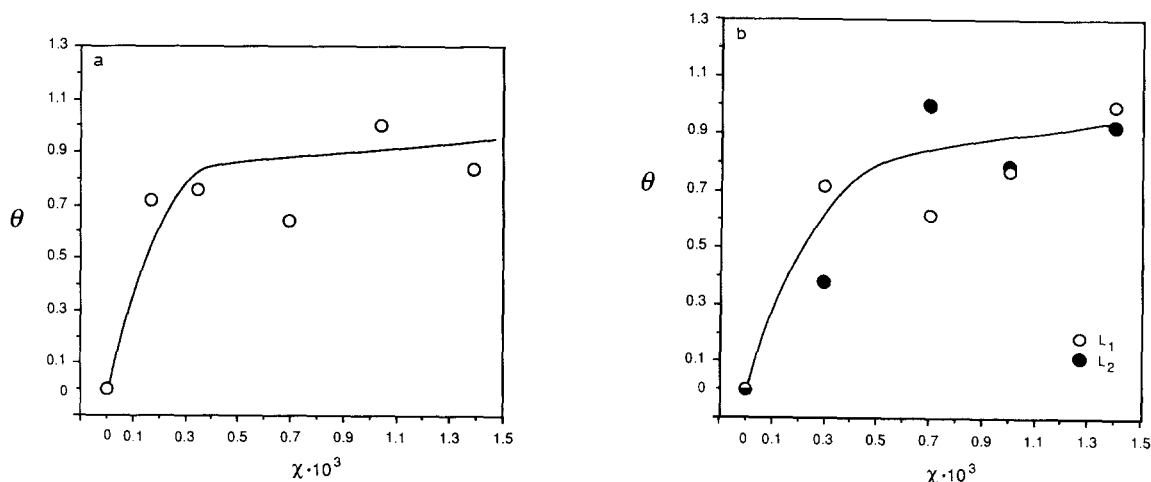


Fig. 7. Degree of surface coverage calculated from the measured growth rates of L-alanine crystals in the presence of (a) L-leucine and (b) L-phenylalanine, and predicted according to the Bliznakov-Langmuir model, Eq. 16.

Table 5  
Influence of additives on the face growth rate of L-alanine

Additive	$r^2$		$b (\times 10^{-4})$		$\Delta G_{\text{ads}} (\text{kcal mol}^{-1})$	
	$L_1$	$L_2$	$L_1$	$L_2$	$L_1$	$L_2$
L-Leucine	–	0.75	–	1.1 (0.5) <sup>a</sup>	–	–5.5
L-Phenylalanine	0.87	0.80	0.7 (0.3) <sup>a</sup>	0.7 (0.4) <sup>a</sup>	–5.2	–5.3

Parameters obtained from nonlinear regression for the growth rate dependence on the additive concentration according to the Bliznakov-Langmuir model (Eq. 4).  $r^2$ , determination coefficient;  $b$ , Langmuir constant; free energy of adsorption  $\Delta G_{\text{ads}} = -RT \ln b$ ,  $R = 1.987 \times 10^{-3} \text{ kcal mol}^{-1} \text{ K}^{-1}$ ,  $T = 298 \text{ K}$ .

<sup>a</sup> Standard deviation ( $\times 10^{-4}$ ).

structural characteristics of the molecules of these additives and the molecular structure of the (011) crystallographic plane this was not expected.

The free energy of adsorption between the additive molecule and the different crystal faces was calculated from the Bliznakov-Langmuir model (Bliznakov and Kirkova, 1957). This model assumes that the growth rate decreases proportionally to the degree of coverage of the crystal surface by additive molecules and that the adsorption of the additive onto the crystal surface is described by the Langmuir isotherm:

$$\frac{1 - \eta}{1 - \eta^0} = \frac{b\chi}{1 + b\chi} \quad (16)$$

The value of  $b$ , the Langmuir constant, was estimated from a weighted nonlinear regression fit of Eq. 16 to the experimental values (Fig. 7a and b). The total free energy for adsorption,  $\Delta G_{\text{ads}} = -RT \ln b$ , obtained from this method is approximately the same for both additives as shown in Table 5. This value is in the range expected considering the kind of interactions that occur at the interface (i.e., hydrogen bonding). There is very good agreement with the  $\Delta G_{\text{ads}}$  values calculated from overall growth rates measured from crystal size distribution analysis (Lechuga-Ballesteros and Rodríguez-Hornedo, 1993b).

AFM photomicrographs of the {120} faces of crystals grown in the presence of additive (Fig. 5b) confirm the results obtained from the growth rate dependence on supersaturation. Even though the roughness of the surface is increased due to the presence of additive, evenly-spaced terraces characteristic of the spiral growth mechanism are observed.

#### 4. Conclusions

In summary, from the kinetic, mechanistic and structural considerations we have found that:

- (i) L-Alanine crystal growth of the {120}, {010} and {011} faces, in both the presence and absence of hydrophobic L-amino acids, follows the screw dislocation mechanism;
- (ii) L-Alanine crystal growth is significantly reduced in the presence of hydrophobic L-amino acids, due to adsorption of the additive onto the surface of the {120} faces of the growing crystal;
- (iii) The effect of hydrophobic L-amino acids on the growth kinetics is explained by assuming that the growth rate inhibition is proportional to the degree of coverage of the additive molecules onto the crystal surface and that their adsorption onto L-alanine crystal faces follows a Langmuir isotherm.

#### Acknowledgments

This work was partially supported by the National Science Foundation (Grant No. CTS-8818627) and by the College of Pharmacy, University of Michigan (Helfman Scholarship). One of the authors (D.L.B.) thanks the Consejo Nacional de Ciencia y Tecnología de México (CONACyT) for the financial assistance received.

#### References

- Addadi, L., Berkovitch-Yellin, Z., Weissbuch, I., Van Mil, J., Shimon, L.J.W., Lahav, M. and Leiserowitz, L., Growth

- and dissolution of organic crystals with 'tailor-made' inhibitors – implications in stereochemistry and materials science. *Angew. Chem. Int. Ed. Engl.*, 24 (1985) 466–485.
- Albon, N. and Dunning, W.J., Growth of sucrose crystals: Determination of edge energy from the effect of added impurity on rate of step advance. *Acta Crystallogr.*, 15 (1962) 474–476.
- Bennema, P. and Gilmer, G.H., Kinetics of crystal growth. In Hartman, P. (Ed.), *Crystal Growth: An Introduction*, North-Holland, Amsterdam, 1973, pp. 263–327.
- Bliznakov, G. and Kirkova, E., Der Einfluß der Adsorption auf das Kristallwachstum. *Z. Phys. Chem.*, 206 (1957) 271–280.
- Bull, H.B., Breese, K. and Swenson, C.A., Solubilities of amino acids. *Biopolymers*, 17 (1978) 1091–1100.
- Burton, W.K., Cabrera, N. and Frank, F.C., The growth of crystals and the equilibrium structure of their surfaces. *Phil. Trans. Roy. Soc.*, A243 (1951) 299–358.
- Chernov, A.A., Formation of crystals in solution. *Contemp. Phys.*, 30 (1989) 251–276.
- Davey, R.J., Mullin, J.W. and Whiting, M.J.L., Habit modification of succinic acid grown from different solvents. *J. Cryst. Growth*, 58 (1982) 304–312.
- Dunning, W.J., Jackson, R.W. and Mead, D.G., The effect of additives on the rate of advance of steps on sucrose surfaces. In Kern, M.R. (Ed.), *Adsorption et Croissance Cristalline*, CNRS, Paris, 1965, pp. 303–316.
- Greenstein, J.P. and Winitz, M. *Chemistry of the Amino Acids*, Vol. 1–3, Wiley, New York, 1961, Vol. 1, pp. 523–568.
- Hartman, P., Structure and morphology. In Hartman, P. (Ed.), *Crystal Growth: An Introduction*, North-Holland, Amsterdam, 1973, pp. 358–402.
- Jackson, K.A., *Liquid Metals and Solidification*, Am. Soc. Metals, Cleveland, 1958, p. 174.
- Lechuga-Ballesteros, D. and Rodríguez-Hornedo, N., Crystal growth and morphology of L-alanine crystals: Influence of additive adsorption. *Pharm. Res.*, 10 (1993a) 1008–1014.
- Lechuga-Ballesteros, D. and Rodríguez-Hornedo, N., Effects of molecular structure and growth kinetics on the morphology of L-alanine crystals. *Int. J. Pharm.*, 115 (1995) 151–160.
- Lechuga-Ballesteros, D. and Rodríguez-Hornedo, N., The relation between adsorption of additives and crystal growth rate of L-alanine. *J. Colloid Interface Sci.*, 157 (1993b) 147–153.
- Lehmann, M.S., Koetzle, T.F. and Hamilton, W.C., Precision neutron diffraction structure determination of protein and nucleic acid components: I. The crystal and molecular structure of the amino acid L-alanine. *J. Am. Chem. Soc.*, 94 (1972) 2657–2660.
- Li, L. and Rodríguez-Hornedo, N., Growth kinetics and mechanism of glycine crystals. *J. Cryst. Growth*, 121 (1992) 33–38.
- Manne, S., Cleveland, J.P., Stucky, G.D. and Hansma, P.K., Lattice resolution and solution kinetics on surfaces of amino acid crystals: an atomic force microscope study. *J. Cryst. Growth*, 130 (1993) 333–340.
- Mathlouthi, M. and Seuvre, A.M., Solution properties and the sweet taste of small carbohydrates. *J. Chem. Soc. Faraday Trans. 1*, 84 (1988) 2641–2650.
- Rodríguez-Hornedo, N. and Wu, H.J., Crystal growth kinetics of theophylline monohydrate. *Pharm. Res.*, 8 (1991) 643–648.
- Schwartz, P.A., Rhodes, C.T. and Cooper, J.W., Solubility and ionization characteristics of phenytoin in normal saline. *J. Pharm. Sci.*, 66 (1977) 994–997.
- Simpson, H.J. and Marsh, R.E., The crystal structure of L-alanine. *Acta Crystallogr.*, 20 (1966) 550–555.
- Weissbuch, I., Addadi, L., Berkovitch-Yellin, Z., Gati, E., Weinstein, S., Lahav, M. and Leiserowitz, L., Centrosymmetric crystals for the direct assignment of the absolute configuration of chiral molecules. Application to the  $\alpha$ -amino acids by their effect on glycine crystals. *J. Am. Chem. Soc.*, 105 (1983) 6615–6621.
- Zipp, G.L. and Rodríguez-Hornedo, N., Phenytoin crystal growth rates in the presence of phosphate and chloride ions. *J. Cryst. Growth*, 123 (1992) 247–254.